v1: 12 November 2024

Research Article

Influence of a City Block on ES-CFD Coupled Analysis

Peer-approved: 12 November 2024

Qeios, Vol. 6 (2024)
ISSN: 2632-3834

Tatsuhiro Yamamoto[1]

1. Architecture and Equipment Engineering, Kurume Institute of Technology, Japan

Coupled analysis using the complementary methods of energy simulation (ES) and computational fluid dynamics (CFD) can improve the calculation accuracy of thermal environment simulations. However, existing studies on ES-CFD coupled analyses that consider the effects of solar radiation and surrounding conditions have been insufficient. In practice, net solar radiation fluctuates, owing to the influence of urban blocks, and the solar radiation incident on the interior determines the heating range of the interior, which results in fluctuations in the convective heat transfer coefficient. This study conducted an ES-CFD coupled analysis to examine differences in the convective heat transfer coefficients due to the different insolation conditions and the surroundings of target buildings. The risk of condensation was evaluated using the dew point temperature in the analysis model, and a neutral insulation performance was employed in the set cases with the presence or absence of urban streets as a variable. Buildings within urban city blocks were observed to have a lower dew point temperature and a higher risk of condensation, which is a reasonable assessment. The results of this study will contribute significantly to the development of comprehensive simulation technologies.

Corresponding author: Tatsuhiro Yamamoto, mech.archi@mechlabo.info

Introduction

Evaluating the environment of city blocks is challenging, and quantifiable data are usually regarded as the most reliable. Wind tunnel experiments are typically used to measure thermal environment data in city blocks. However, defects in the data of wind speed distribution in the vertical direction of high-density urban boundary layers were determined in a wind tunnel experiment[1], which showed a discrepancy between the wind tunnel experimental data and actual phenomena. The study used measured wind data to provide a reference for the conditions of the wind tunnel experiment; therefore, it is not sufficient to rely only on experiments[2]. Another study evaluated the distribution of shade at various temporal and spatial resolution in a street in a suburb of Sydney, Australia. The authors used electronic sun journal data and evaluated the shade distribution and profiles by time zone[3]; such data are valuable because sunlit and shaded surfaces are important elements used in thermal load calculations.

Interest in ventilation has increased recently owing to the COVID-19 pandemic. While studies on passive ventilation are still being conducted from the viewpoint of energy savings[4], many studies on ventilation in relation to polluting materials have also been conducted[5][6][7] and a study on ventilation in relation to heat exposure has also been reported[8]. As such, studies on ventilation are currently being conducted based on different perspectives. Since studies related to COVID-19 are highly valued, those relating to preventing droplet infection[9] and those specific to sports events[10] are of particular interest. Outdoor temperature is an important factor associated with ventilation; research on solar cells and PCM (phase-change material) has gained attention because they are significantly affected by the shadow of city blocks[11][12], and an ES program specific to the influence of shade has also been developed[13]. However, although several studies on the effects of solar radiation have been conducted, it is also necessary to consider ventilation in conjunction with the thermal environment. If the findings of such studies are compiled into a database, designers can introduce advanced thermal environment simulations in the basic design phase.

 doi.org/10.32388/GV07BN.2

Studies of the thermal environment of an urban area are closely related to the wind conditions of the urban environment. Computational fluid dynamics (CFD) can thus be used to examine various segments of the city[14]. Understanding the passage of wind from outdoors to indoors is important for design practice, and city blocks and the interiors of buildings should not be considered as separate entities, and Wu et al.[15] thus evaluated the continuous wind environment from the surrounding city block to the interior of buildings. CFD is suitable for examining the temperature distribution in offices and houses; however, it divides space into meshes (cells) and solves discretized partial differential equations (potentially involving millions of algebraic equations), which makes each iteration computationally intensive. Studies using CFD have been conducted to examine problems related to the reduction of calculation loads[16][17]; however, analyzing the resulting data is difficult using personal computers (PCs) designed for business use in building design. When designing city blocks using CFD in urban environmental engineering, the computational resources are large at scales of around 10 million meshes, but using a supercomputer to perform these calculations is unfeasible. Moreover, high-load calculations (such as LES) have been conducted, but advanced knowledge is required to use them in practice; therefore, the Reynolds-Averaged Navier-Stokes (RANS) is recommended[18]. Energy simulations (ESs) are also used in the thermal examination of the interior of a building. Alajmi et al.[19] obtained the results of the long-term unsteady calculations by integrating the Air Conditioning System Simulation into an ES to assess and examine the thermal environment inside the building. Using an ES is essential for reducing calculation loads. However, because ES represents space in terms of mass, it is not suitable for calculating spatial distributions such as velocity or temperature.

Zhai and colleagues developed and established ES-CFD coupled analysis as one such analytical technology[20][21][22]. Coupled ES-CFD analysis is a computational technique that interpolates the advantages and disadvantages of ES and CFD. It is an extremely complex method that requires familiarity with heat transfer theory and CFD. Many studies have been conducted on the interior environments of rooms to examine the accuracy of unsteady analysis for thermal environment estimation[23]. Following case studies of offices, coupled analysis (including that of facility equipment) has become well employed[24][25]. Recently, studies using ES-CFD coupled analysis have been conducted on a city scale[26], and comfort has been examined by coupling the advection quantity between zones[27]. The objects of analysis have included areas belonging not only to the field of architecture but also to greenhouses. A case study on greenhouses revealed that the temperature of the sky and the degree of opening of the ventilation device influenced the convection heat transfer coefficients, and the optimum operation method was suggested based on climate[28]. Therefore, this technology is now being introduced to various fields instead of its previous use focusing only on indoor thermal environments.

Several methods have been proposed to conducting coupled analyses in cities, and some focus on outdoor convective heat transfer coefficients and microclimate[29]. In addition, the number of meshes required for the model on CFD has been examined to reduce the load of CFD-ES coupled analysis for the outdoor environment[30]. Therefore, technology in this field is continually evolving. Kawai et al.[31] examined the coupling of ES and calculations for a room considering the long-wave radiation of the city block and the reflective sunlight from the ground. However, ES-CFD coupled analysis was not conducted in this study. Obtaining an accurate convective heat transfer coefficient is particularly important for ES-CFD coupled analysis. It is currently possible to simulate an urban block as a component of a transient system simulation tool[32], a type of ES, and to consider the influence of direct and sky insolation on the exterior wall and that of transmissive insolation through glasses on sunlit and shaded surfaces. Studies have used the surrounding weather conditions as input conditions, including some studies that intend to use weather data in the near future[33][34]. Knowledge of meteorological data as an input condition for ES and crucial for ES-CFD coupled analysis. Although reference year weather data are usually used, typical and design weather year data for were recently included in the building design, and this improved the load of cooling and heating twofold. In addition the accurate maximum load of cooling and heating were successfully estimated[35]; this estimation used near-future weather data, and it was confirmed that the wet bulb globe temperature increased by 1.11°C on average. Therefore, it is crucial to use weather data when modelling urban environments, and the thermal environment of the room should also be considered. Using the weather data for a city, Tang et al.[36] created urban (Typical Meteorological Year) TMY (uTMY) data, which correspond to the actual weather data of the city block. When the annual energy demand was calculated using uTMY, the resulting value was 24% less than that obtained using TMY. These weather data are thus valuable input conditions for ES, but these do not represent the microclimate around individual buildings; therefore, more employing specific validation data is desirable.

This current study aimed to conduct an ES-CFD coupled analysis focusing on the thermal environment of a room while considering the surrounding city block. In this study,

a city block was first simulated; a house was subsequently simulated and placed in the middle of the city block. Thereafter, the influence of the ES-CFD coupled analysis with and without city blocks was investigated. Due to the divergent discussions in this study, we decided to use the extended AMeDAS (Automated Meteorological Data Acquisition System) weather data for the standard year to represent the weather data. This study focused on a comparative examination based on the results of the steady-state analysis at the time of culmination and will be developed in phases. The results of this study will contribute significantly to the development of comprehensive simulation technologies for rooms in city blocks.

Materials and Methods

The calculation of the convective heat transfer coefficient was an important factor in this study. Equation (1) was used to calculate the heat flow, which employs a velocity scale based on the shearing stress and precisely expresses the influence of vector components to reflect the heat flow,

$$q_{wall} = \frac{\rho_f\,(y_c) \bullet C_{P,f}\,(y_c) \bullet u_\tau}{T^+\left(y^+_{fluid}\right)}(t_{wall} - t_{fluid}\,). \quad (1)$$

The transformation of Equations (1) and (2) based on Newton's law of cooling is expressed,

$$h_c = \frac{q_{wall}}{(t_{object} - t_{fluid}\,)}. \quad (2)$$

In Eqs (1) and (2):

q_{wall}: wall heat flux (W/m^2); P_f: density of the fluid (kg/m^3); y_c: normal distance from the wall (m); u_r: velocity scale based on wall shear stress (m/s); T^+: dimensionless temperature (-); y^+_{fluid}: dimensionless distance (-); t_{wall}: surface temperature of wall (K) and t_{fluid}: fluid temperature (K).

The definition of the reference temperature is important for the convective heat transfer coefficient. In this study, the dimensionless distance, y$^+$, was used to define the reference temperature for turbulent waters based on Prandtl's wall law. In addition, as shown in Equation (1), the wall viscosity effect was considered using a velocity scale based on the shear stress.

Equation (3) expresses the heat balance of space and shows that the convective heat transfer coefficient is an important element,

$$V_o\overline{c\gamma}\frac{dT_i}{dt} = \sum_{j=1}^{J} S_{i\,,\,j}\,h_{i.j}\left(T_{i\,,\,j} - T_i\right) + V_o c\gamma\,(T_o - T_i), \quad (3)$$

in which V_o: amount of outdoor air introduced [m^3/s] $\overline{c\gamma}$: apparent heat capacity of the room including furniture [J/m^{3}K]; $S_{i,\,j}$: area of target surface j [m^2]; $h_{i,\,j}$: convective heat transfer coefficient at target surface j [W/m^{2}K]; $T_{i,\,j}$: temperature of target surface j [K] and *cy*: volume specific heat [J/m^{3}K].

Method of coupling

Figures 1(a) and (b) show a schematic flow representation of the coupled analysis. CFD is performed by the finite volume method, using a set of continuity, motion, and energy equations.ES, on the other hand, allows for transient calculations by connecting the entire building with nodes, solving the matrix of each element, and letting time advance. When buildings are present around the target building, both sunlit and shaded areas are observed inside the room and on the outdoor surfaces. In STEP 1, the influence of the sunlit and shaded sides was calculated using the AMeDAS data. The amount of solar radiation incident on the wall and glass surfaces was calculated and used as the boundary condition to estimate the transmissive heat flow and amount of solar transmission. In STEP 2, the indoor thermal environment was calculated based on the obtained surface heat flux inside the room. The calculations were performed using the presence or absence of urban streets as a variable. In STEP 2.5, the data of outdoor air temperature and relative humidity from the AMeDAS meteorological data were considered the boundary conditions for the CFD. In this case, because the convective heat transfer coefficient was unknown, a value of 4 W/m^{2}K was used. This value is idiomatic.

The surface temperature of the room calculated here was passed to the CFD, and the convective heat transfer coefficients and the amount of advection between zones were calculated (STEP 3). The calculated physical quantity was then passed to the ES, and the indoor thermal environment was again estimated. No further calculations were necessary for the relative evaluation (STEP 4). However, for evaluating the dew condensation risk, the recalculated surface temperature of the ES was passed to the CFD (STEP 5), and comfort was evaluated using the ES.

The time zone difference was limited to the natural convection field without forced convection. Therefore, if the convective heat transfer coefficient was used at around noon when the maximum amount of sunlight enters the room, any potential major problem could be avoided. The thermal insulation performance was comparatively analysed. The results of the calculations for single- and double-room houses were compared to examine the influence of transmissive heat flow and the influence on the surface receiving heat by solar radiation.

As a phased examination was required, the influences of opposite long-wave radiation and isolation reflected by the

ground were not considered. This study conducts a relative evaluation, which has not been previously attempted in other studies. Therefore, the convective heat transfer coefficients outside the room, which represent the microclimate, were not estimated using CFD analysis because they were examined in a stepwise manner. Solar radiation enters the ground surface and the wall of the opposing residence, which it reflects off and ultimately enters the subject building. We believe it is important to lay the groundwork for a coupled analysis to account for re-radiation from the opposing house, but this is not the focus of discussion in this study.

doi.org/10.32388/GV07BN.2

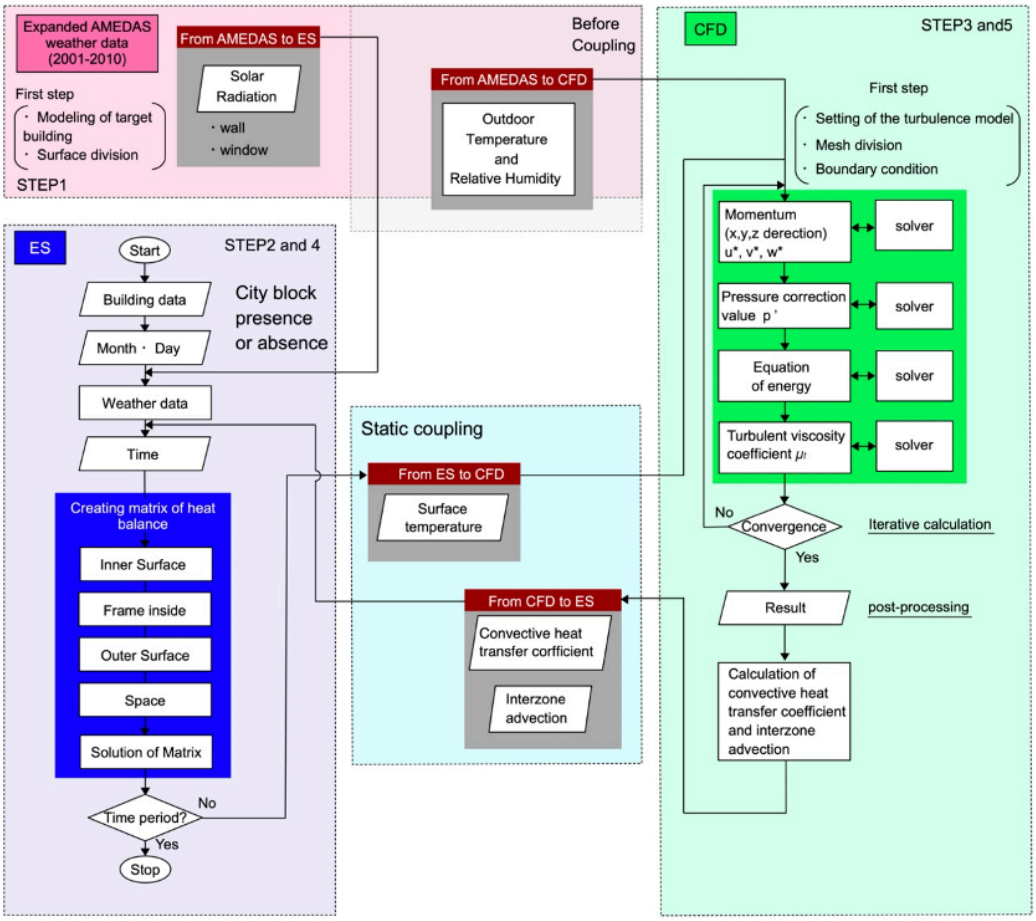

Figure 1a. Schematic flow representation of the coupled analysis. ES and CFD coupled analysis flow[37]

doi.org/10.32388/GV07BN.2

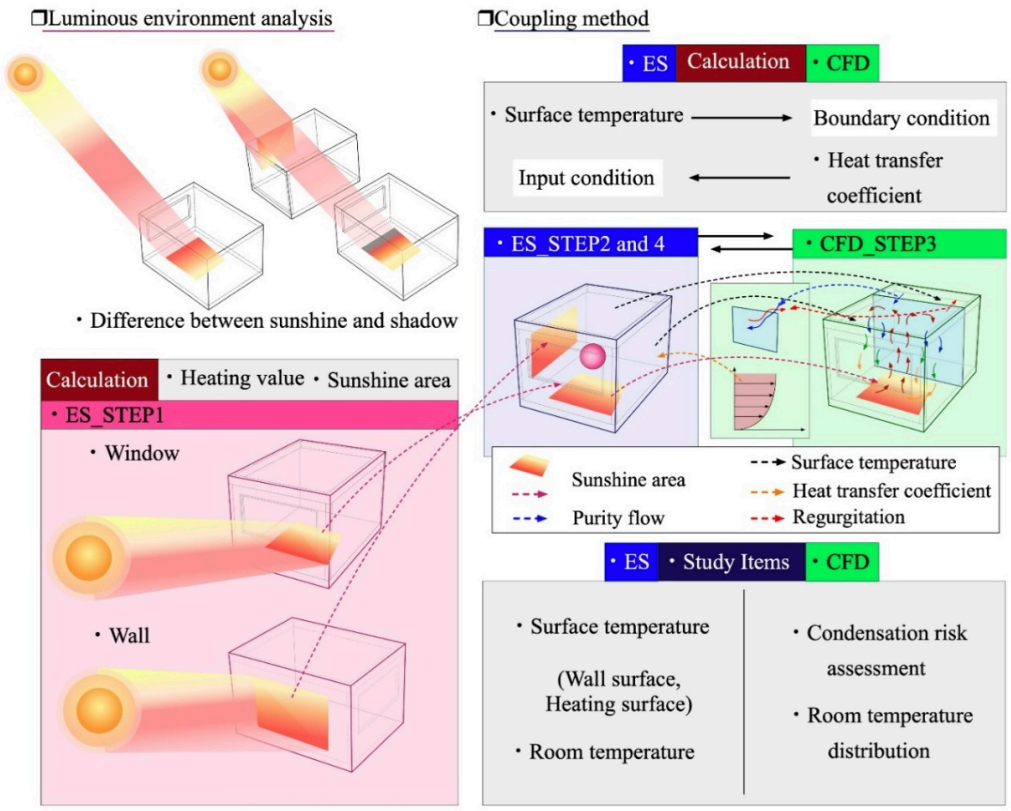

Figure 1b. Schematic flow representation of the coupled analysis. Coupled analysis flow with diagram.

Note: The presence or absence of an urban district as a foundation was considered in the static coupling process. Furthermore, the boundary input conditions for ESs with and without city blocks were devised.

Description of target building

Figure 2 presents the models used in this study. The ES and CFD analysis models are shown in Figure 2(a), where the model perfectly represents an actual building. A virtual wall was installed in the middle of the building to calculate the advection current between zones using CFD, and the calculation results were passed on to the ES. A window was set on the south side, where the sun culminated at noon. The model of the building was simulated to conduct a basic examination and simplify the analysis. Figure 2(b) shows the simulation of neighbouring buildings and streets based on Japan's Building Standard Law[38]. The analysis was conducted within the bounds of common sense. The target building had one storey because this is a basic study; if a two-storey building or higher had been used, the results would have been more complex. This results of this study relate solely to the simulation results, and no other experiments were conducted. As the study was conducted to assess the modelling an urban area, preparing a simplified analytical model and conducting a basic study was considered to be more important than reproducing the actual environment.

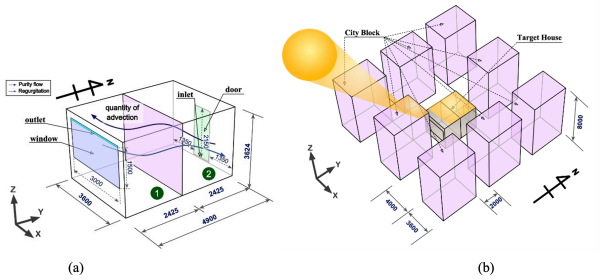

Figure 2. Analytical models used in this study. (a) ES-CFD analysis model. (b) City block model.

Contents of analysis and conditions for case studies

Table 1 lists the wall compositions of the cases studied. A 12-mm plywood was placed on the exterior and interior surfaces of the ceilings and walls, and a 10-mm float was

doi.org/10.32388/GV07BN.2

used for all window surfaces. The floor was insulated with a 12-mm XPS between 12-mm plywood boards. Cases 1, 2, and 3 used simple heat insulators and winter and summer seasons were assumed. Situations with and without urban blocks were examined for each case. The relationship between the change in the dew point temperature and room temperature with and without the city block was analysed in Case 2, which represented all cases. The analytical results of single-room and two-room conditions were compared to deepen our understanding of employing ES-CFD coupled analysis. Note that Cases 2-1-1 and 2-2-1 indicate, respectively, whether or not condensation was evaluated; in Case 2-1-1, the dew point temperature distribution was not evaluated, but it was evaluated in Case 2-2-1. We hypothesized that the risk of condensation on the interior wall body surface would be higher depending on the presence or absence of an urban district; therefore, a condensation risk assessment of the wall surface temperature was added. Another reason for assessing the condensation risk in the summer season was that Japan is more humid in the summer season, which could result in a condensation risk when the area is shaded. This study discusses the presence or absence of condensation risk rather than showing that condensation risk occurs.

Item	Case 1		Case 2		Case 3	
Wall insulation (mm)	No insulation Thermal		Glass wool 40 Thermal conductivity: 0.039 [W/mK]		Glass wool 80 Thermal conductivity: 0.039 [W/mK]	
-	Case 1-1	Case 1-2	Case 2-1	Case 2-2	Case 3-1	Case 3-2
	City block					
Summer* (Two rooms and one room)	N	Y	N	Y	N	Y
Winter* (Two rooms and one room)	N	Y	N	Y	N	Y
-	-	-	Case 2-1 (A)	Case 2-2 (B)	-	-
Dew point temperature* (Two rooms and one room) In Summer	-	-	N	Y	-	-

Table 1. Wall composition and cases examined in this study

* Letters and symbols in these rows indicate the following: 'Y' indicates that the item in the left column is considered in the case study;'N' indicates that the item is not considered; and '–' indicates that none of the letters are applicable.

Analytical conditions of ES-CFD coupling

The conditions of ES-CFD coupling are shown in Table 2. TRNSYS was used for the ES analysis. The direction was set such that the sun culminated at noon for the analysis model. Thus, an unsteady calculation of a comfort index, such as the PMV (predicted mean vote), was performed on the safe side. The night-time condition was unlike the actual phenomenon, as no solar radiation entered at night. Therefore, the PMV was examined at a time during the day. The date and time were chosen to match the day with the highest temperature in summer and that with the lowest temperature in winter. For advection between the zones, a commonly used value of 20 ventilations per hour was used as input for the initial condition. The frequency of ventilation was set to 0.5 ACH based on the Building Standard Act of Japan. The frequency of ventilation refers to the number of times the air in a room is replaced per hour.

doi.org/10.32388/GV07BN.2

Software for analysis	TRNSYS.Ver.18	
Date and time	Winter	At noon on 9th January
	Summer	At noon on 5th August
Location	Tokyo	
Weather data	Expanded AMeDAS weather data (2001–2010)	
Ventilation	nil	
Preliminary calculation period	7 days	
Interval of calculation time	One-minute interval	
Advection quantity between zones	Ventilated 20 times	
Ventilation frequency	0.5 ACH（Times / hour）	

Table 2. Conditions used to calculate TRNSYS

Table 3 lists the analytical conditions for CFD. The STAR-CCM+[39] was used as the computational software for conducting CFD. A basic study requires precise calculations; therefore, the area near the walls was carefully considered when calculating convective heat transfer coefficients, and a low-Reynolds-number turbulence model was thus used for analysis. The calculation was conducted assuming that outdoor air flowed in through the door gap. The length scale was set to 1/7th of the slit width; the turbulence intensity was set to 0.01; the inflow rate was set to flow at 0.5 time/h in winter and summer; the outdoor air temperature was kept stable, regardless of the presence of a city block; and the outdoor air temperature at noon, which was the sun culmination time, was referred to for this. Mesh division was performed to achieve $y+ < 1$.

doi.org/10.32388/GV07BN.2

Item	Conditions		
CFD code	STAR-CCM+[39] 12.04.011		
Turbulence model	Standard k-ε low-Re model[40]		
Mesh number	Approximately 4 million meshes, y+ < 1		
Walls and heat sources	Calculated values [K]		
	Velocity: no-slip, $k\|_{wall}$: no-slip $\varepsilon = \frac{2vk}{y^2}$ k: von Karman's constant ()		
Inflow conditions	$k = \frac{3}{2}(Iv)^2$ $\varepsilon = \frac{C_\mu{}^{3/4}k^{3/2}}{L}$ L: 0.129 [m] (1/7 of the slit width) v: wind speed [m/s] C_μ: model coefficient () k: kinetic energy [m^2/s^2] I: turbulence intensity () ε: turbulence dispersion rate [m^2/s^3]		
	Turbulence intensity	0.01 ()	
	Winter	Inflow temperature	7.99 [°C]
		Flow rate	0.011 [kg/s]
	Summer	Inflow temperature	34.80 [°C]
		Flow rate	0.011 [kg/s]
	Outlet	Pressure outlet [0 Pa]	

Table 3. Conditions for calculating computational fluid dynamics in this study

Results of Analysis

The chronological changes in the outdoor temperatures and insolation in summer and winter on the days during which the calculations were performed are shown in Figure 3. Temperatures dropped gradually until 08:00 and reached their highest levels in the daytime and evening in both summer and winter. A similar tendency was observed for the amount of insolation. As the analytical results of this study were significantly affected by the outdoor temperature, it was necessary to examine multiple elements.

doi.org/10.32388/GV07BN.2

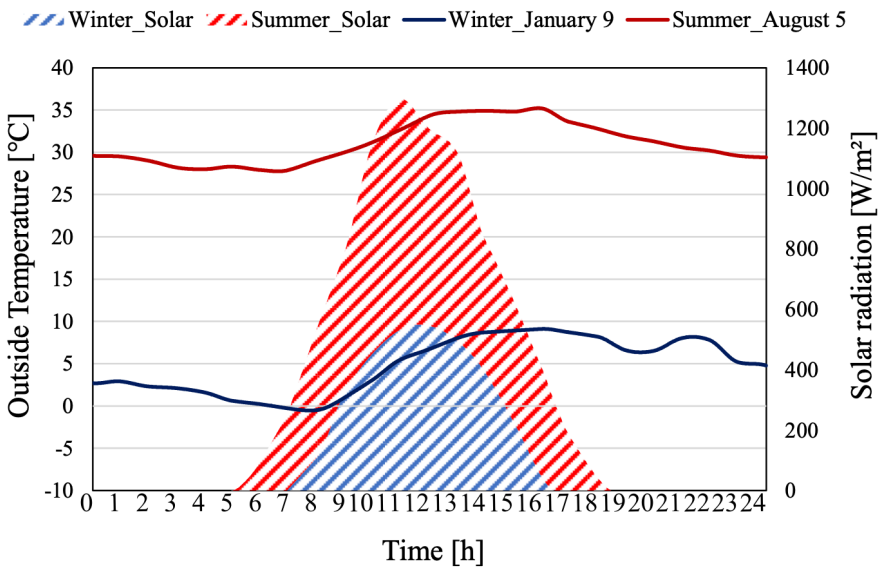

Figure 3. Chronological change in outdoor temperatures in summer and winter on days on which calculations were performed

Figure 4 shows the comparison of global solar radiation with and without a city block. In winter, the solar radiation on the south wall and window was as high as 800 W/m^2 without a city block because of the low solar azimuth during winter. The solar radiation on the roofs with a city block in winter was 150 W/m^2, which was lower than that on the roofs without a city block. No significant difference was observed in the heat received on the roofs for Zones 1 and 2 in winter.

There was no major difference between solar radiation on the surfaces, except for the south wall and window, between the buildings surrounded by a city block and those that were not. In summer, solar radiation reached only approximately 300 W/m^2 on the south surface of the building without a city block because of the high altitude of the sun, but radiation on the roofs showed a higher value of approximately 680 W/m^2 in summer than in winter. The solar altitude is high in the summer; therefore, solar radiation on the roofs of the building with a city block was similar to that without a city block. The solar radiation on each part of the building without a city block in summer differed by approximately 50 W/m^2 compared to that in winter, except for that on the southern surface and floors.

doi.org/10.32388/GV07BN.2

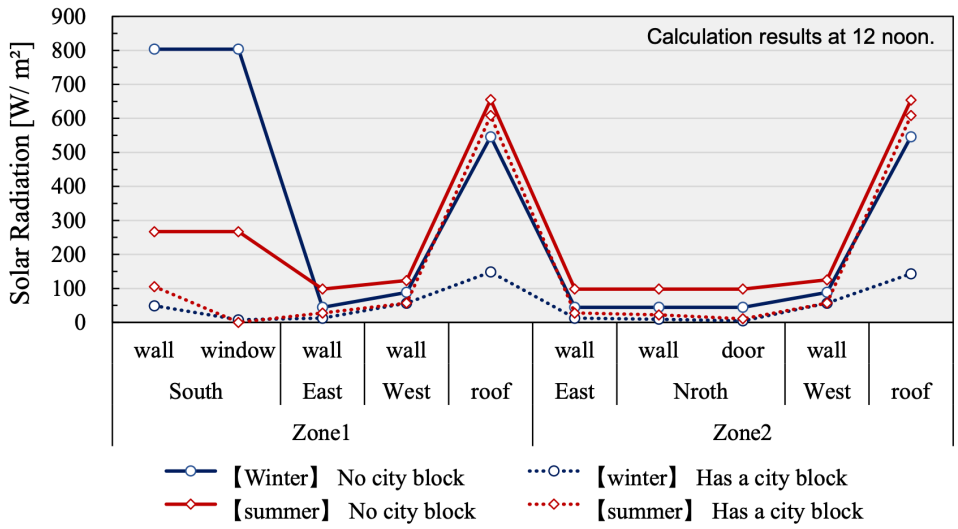

Figure 4. Solar radiation on parts of the building with and without a city block

Figure 5 shows the transfer rates between the zones in winter and summer. The transfer rates between zones were lower in summer than in winter because the wall surface temperatures were similar to the outdoor temperature, and because the increase in surface temperature owing to solar radiation is more influential in winter. In the absence of city blocks around the building, the transfer rate increased significantly. The rate reached approximately 1000 m^3/h in Case 3-1 with increasing insulation performance. We assumed that the high indoor surface temperature caused by the high insulation performance and the decrease in the surface temperature in Zone 2, which did not receive heat from solar radiation, generated buoyancy in the room.

The total values show the sum of pure flow and reverse flow from Zone 2 to 1. CFD ventilation is modelled such that outdoor air flows in through the gap under the door of Zone 2, whereas the gap above the window in Zone 1 works as an exit through which the air is pressurised to go through.

doi.org/10.32388/GV07BN.2

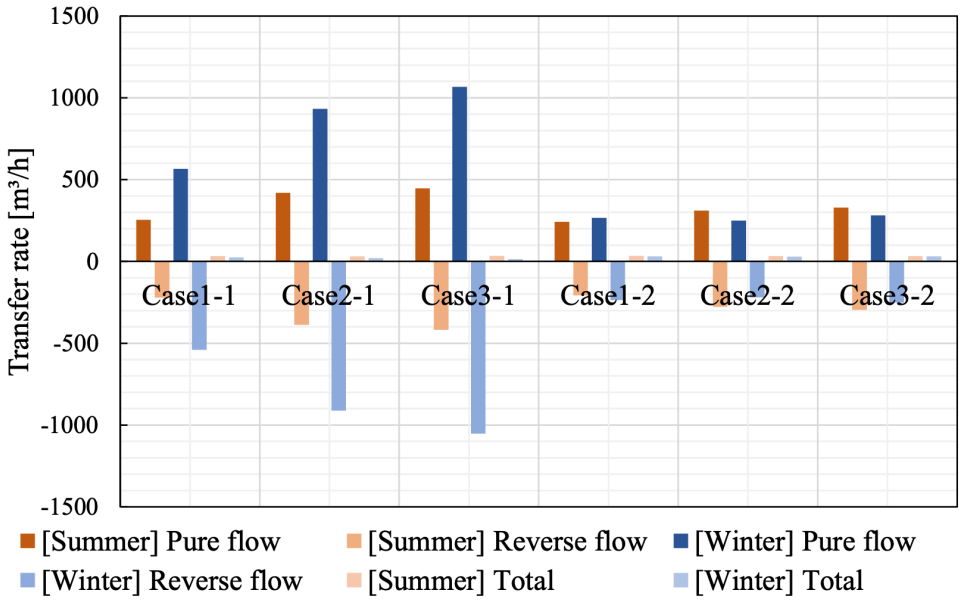

Figure 5. Transfer rate between zones in summer and winter

Further analysis of differences between winter and summer

Figure 6(a) shows the surface temperatures inside the room and convective heat transfer coefficients of the building without a city block in winter. In Zone 1, near the window, the higher insulation performance tended to make surface temperatures higher inside the room, and we assumed that multiple reflections of radiation caused high surface temperatures in the room. In Zone 2, the lower insulation performance caused relatively higher surface temperatures (approximately 10 °C) in the room.

For Cases 2-1 and 3-1, surface temperatures were lower than air temperatures, which indicate that the outdoor air had a stronger effect when the insulation performance was low. This trend is observed in ZONE 1, while the wall surface temperature in ZONE 2 has a lower value. On the other hand, the reason for the lower wall surface temperature in ZONE 2 is that the effect of multiple reflections after the solar radiation passes through is only reflected in ZONE 1. When outdoor air was introduced, the room temperature (and consequently the surface temperatures in the room) decreased. The outdoor air temperature dropped below 0°C at night (20:00). Although the window performance was the same for both cases, the case with highly insulated wall structures was strongly influenced. The convective heat transfer coefficients tended to be higher for cases with higher insulation performance. In other words, the case with higher insulation performance showed higher levels of pure and reverse flows between the zones. Therefore, we assumed that the insulation performance significantly influenced the velocity scale based on the shearing stress near the wall surfaces.

Figure 6(b) shows the surface temperatures in the room and convective heat transfer coefficients of the building with a city block in winter. The wall structures without an insulator exhibited higher temperatures than those with insulators for both Zones 1 and 2. The outdoor air temperature was below 0°C at 20:00. Because of the strong influence of heat flow through the window and the high performance of the insulator, the room temperature did not rise when the outdoor air temperature increased. The convective heat transfer coefficients of the wall surfaces were 1–2 W/m^{2}K except for those with a window and north door. Therefore, the convective heat transfer coefficients were affected by advection between zones. Although the insulation of the window surface showed a high performance, the value of the convective heat transfer coefficient was low. We assumed that circulation flows were generated and that the difference between the reference and window surface temperatures was small owing to the influence of low temperatures on the wall surface.

With respect to the analytical results for the building in winter without a city block, both the surface temperatures and convective heat transfer coefficients were lower for the one-room building than for the two-room building,

doi.org/10.32388/GV07BN.2

and this was attributed to the solar transmission that entered Zone 1, which was levelled. In contrast, for the cases with a city block, there were no significant differences between the room temperature or convective heat transfer coefficients of the one- and two-room buildings. These results show that a trend exists for Zone 1 but not for Zone 2, and they illustrate the computational limitations of the current ES tool. As the validation in this study is based on relative comparisons, no major problems arise concerning the research objectives.

Although no significant influence was recognised when considering a city block, dividing the space into two rooms proved better in some cases.

Figure 6(c) shows the change in surface temperatures and convective heat transfer coefficients without a city block in summer, where the surface temperatures reached 40°C. Surface temperatures tend to decrease with the use of high-performance insulators. Unlike in winter, there was no difference between the outdoor air temperature and the surface temperature in summer. Therefore, the insulation performance of the window, which was the same for all cases, did not contribute significantly to the surface temperature. The convective heat transfer coefficients were approximately 1 W/m^{2}K lower than those in the winter. The advection between zones in summer was lower than that in winter, which contributed to the lower convective heat transfer coefficient values.

The change in surface temperatures and the convective heat transfer coefficients for the building with a city block in summer (Figure 6(d)) shows a difference of only approximately 10°C compared with the cases without a city block. This phenomenon is influenced by the significant difference in the advection between zones, which was caused by the temperature difference of approximately 20°C in Zone 1 during winter.

With respect to the analytical results for summer, the surface temperatures of the one-room building without a city block corresponded to the levelled values of the surface temperatures of the two rooms. However, the convective heat transfer coefficients of the one-room building were lower than those of the two-room building. In the case of the one-room building within a city block, the surface temperatures tended to be higher than those of the two-room building. This finding can be attributed to the significant influence of heat transmission from the window surface on the one-room building. No significant difference was present between the one-room and two-room buildings regarding the convective heat transfer coefficients of the building with a city block.

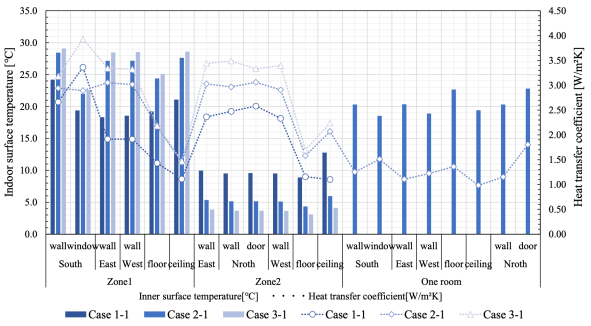

(a)

Figure 6a. Results of calculation of boundary conditions for the room and building in winter and summer. Surface temperatures inside the room and convective heat transfer coefficients of the building (a) without a city block in winter, (b) with a city block in winter, (c) without a city block in summer, and (d) with a city block in summer.

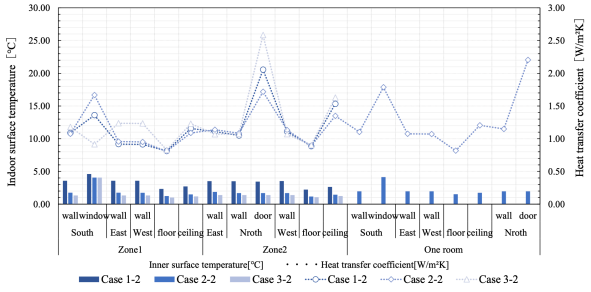

(b)

Figure 6b. Results of calculation of boundary conditions for the room and building in winter and summer. Surface temperatures inside the room and convective heat transfer coefficients of the building (a) without a city block in winter, (b) with a city block in winter, (c) without a city block in summer, and (d) with a city block in summer.

doi.org/10.32388/GV07BN.2

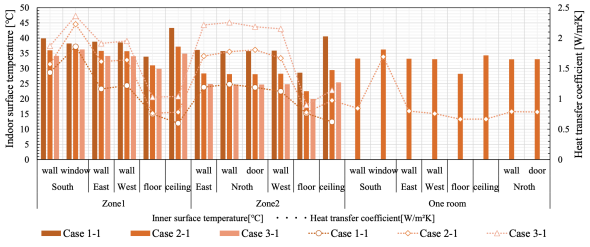

(c)

Figure 6c. Results of calculation of boundary conditions for the room and building in winter and summer. Surface temperatures inside the room and convective heat transfer coefficients of the building (a) without a city block in winter, (b) with a city block in winter, (c) without a city block in summer, and (d) with a city block in summer.

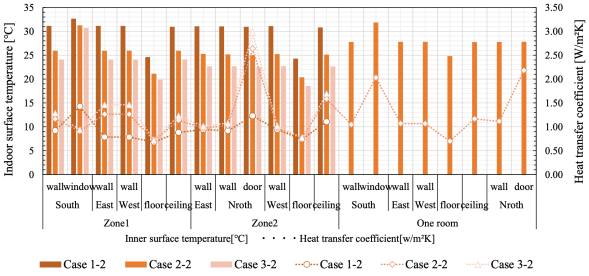

(d)

Figure 6d. Results of calculation of boundary conditions for the room and building in winter and summer. Surface temperatures inside the room and convective heat transfer coefficients of the building (a) without a city block in winter, (b) with a city block in winter, (c) without a city block in summer, and (d) with a city block in summer.

Analysis of the difference in room temperature with and without ES and CFD coupling

Figure 7 shows with and without coupling (with STEP4, without STEP2) the change in convective heat transfer and room temperature. of convective heat transfer coefficient at 12:00 when coupled ES and CFD are performed.

The convective heat transfer is described in Equation [4] as the convective heat transfer coefficient of each wall in Equation [3] multiplied by the difference between the temperature of the wall and the bulk temperature of the room, which is calculated using ES. This equation indicates the heat supply of the ES from the indoor wall surface to the indoor space in each zone,

doi.org/10.32388/GV07BN.2

$$q_{wall\_ES} = \sum_{n=1}^{6} h_{wall\_zone1} \bullet A_{wall_{zone1}} \left(t_{wall_{zone1}} - t_{bulk_{zone1}}\right) + \sum_{i=1}^{6} h_{wall_{zone2}}, \bullet A_{wall\_zone2} \left(t_{wall\_zone2} - t_{bulk\_zone2}\right) \quad (4)$$

in which q_{wall_ES}: thermal loss of indoor wall surface of ES; h_{wall_zone1}: n-th convective heat transfer coefficient of Zone 1 (W/m^{2}K); A_{wall_zone1}: n-th wall surface area of Zone 1 (m^2]; t_{wall_zone1}: n-th wall surface temperature of Zone 1 (K); t_{bulk_zone1}: Bulk temperature of Zone 1 (K); h_{wall_zone2}: i-th convective heat transfer coefficient of Zone 2 (W/m^{2}K); A_{wall_zone2}: i-th wall surface area of Zone 2 (m^2) and t_{bulk_zone2}: Bulk temperature of Zone 2 (K).

As shown in Figure 7(a), the convective heat transfer increased in both winter and summer as the insulation performance improved, which is consistent with the results shown in Figure 7(b). Room temperatures decreased in winter and increased in summer because the amount of convective heat transferred was low. This phenomenon could have affected the heat received via solar radiation from the window surface. Simultaneously, we assumed that heat generated by the outdoor air was transmitted from the outdoor wall and window surfaces. The amount of convective heat transfer before and after coupling differed significantly. For each case, the amount after coupling decreased by approximately 1000 W in winter and 400 W in summer compared with that before coupling. However, in cases with a city block, the convective heat transfer values were positive. After coupling, temperatures tended to increase in cases with a city block in both winter and summer. Generally, the temperature rose more than 1 °C; the temperature increase was caused by the change in convective heat transfer, which contributed to the room temperature. Particularly in summer, the cases with a city block were strongly influenced by radiation generated by the heat received from solar radiation.

With respect to the analytical results for the one-room building without a city block, the convective heat transfer value was low at approximately 700 W before coupling, as the difference between the initial room temperature and the temperature of the wall surface was small, which affected the room temperature. A significant difference was present between the indoor temperatures of the one- and two-room buildings.

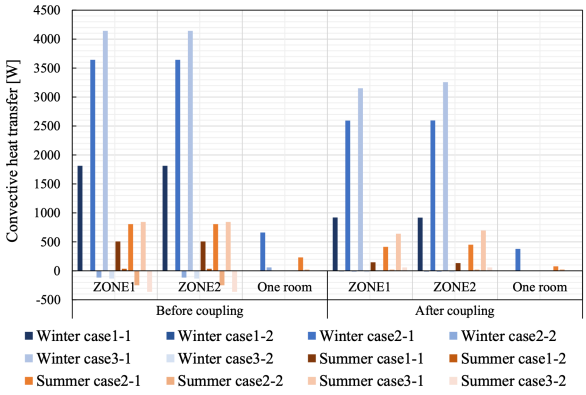

(a)

Figure 7a. Difference in (a) convective heat transfer and (b) room temperatures among the cases before and after coupling

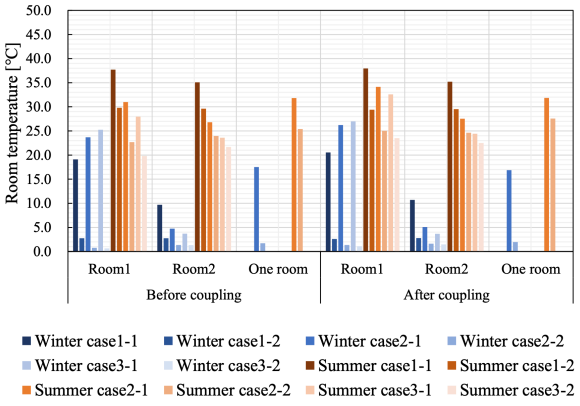

(b)

Figure 7b. Difference in (a) convective heat transfer and (b) room temperatures among the cases before and after coupling

The reason for the difference between the surface temperatures of the two- and one-room buildings was examined in Cases 2-1-1 and 2-1-2.

The saturated vapour pressure was calculated using Equation (5), the vapour pressure can be expressed by Equation (6) when the relative humidity is known, and the dew point temperature can then be calculated using

doi.org/10.32388/GV07BN.2

Equation (7) with constant values (*A*: 6.116441(), *m*: 7.591386 (-), and T_n: 240.7263 (K] in the range of temperature between 120 and +50 (°C) and a vapour pressure of P_w(hPa],

$$P_{ws} = A \bullet 10^{(\frac{m \bullet T}{T+T_n})}, \quad (5)$$

$$P_w = P_{ws} \bullet RH/100, \quad (6)$$

$$Td = \frac{T_n}{\left[\frac{m}{10\log\left(\frac{P_w}{A}\right)} - 1\right]}, \quad (7)$$

in which P_{ws} is the saturated vapour pressure (hPa); P_w is the vapour pressure (hPa); RH is relative humidity (%); T_d is the dewpoint temperature (℃); T is absolute temperature (K) and T_n is the triple-point temperature (273.16 [K]).

The dew condensation risk for the two- and one-room buildings without a city block for Cases 2-1-1 and 2-2-1 was evaluated, as shown in Figures 8 and 9. Comparing the temperature change in a building without a city block to that with a city block, the temperature stratification was evaluated for the two-room building. Although a similar trend was observed for the one-room building, the results showed that the temperature of the building without a city block was slightly higher than that with a city block. We assumed that the surface temperature increased solely because it was significantly influenced by the heat influx from the window surface as a result of being divided into zones. The velocity that shows the maximum value of 0.4 m/s conforms to the temperature and dew point temperature distributions.

Comparing the conditions of the buildings with and without a city block, the dew point temperature of the two-room building with a city block was slightly higher than that without a city block. However, the distribution did not differ significantly. This phenomenon was caused by the higher surface temperature of the boundary condition of the one-room building than that of the two-room building when the building was surrounded by a city block. The results showed that the dew condensation risk was high in buildings without a city block, according to the correlation between temperature distributions.

Lower dew point temperatures and a higher risk of condensation occured when there are no street walls, but this was due to the higher indoor temperatures. In addition, the wall surface temperature was more strongly influenced by heat penetration on the wall surface and solar radiation transmission on the window surface when there were no city blocks.

The dew point temperature was higher when there was a street section, and the risk of condensation was lower. This could have been due to lower indoor temperatures and the reduced condensation risk. However, the relationship between condensation and the wall surface temperature is not considered in this study.

These findings indicate the importance of including a city block in simulations. More precise data can be obtained if the microclimate is also considered. However, we did not include climatic information, as this study was relative and comparative.

	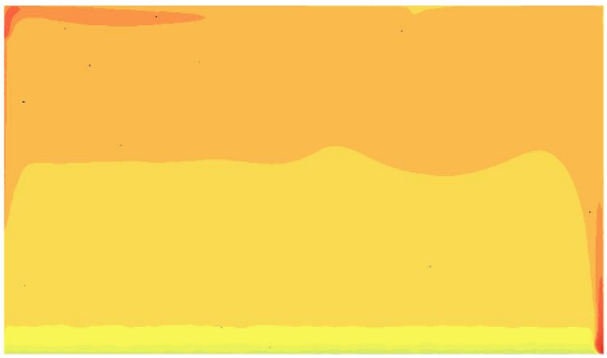

doi.org/10.32388/GV07BN.2

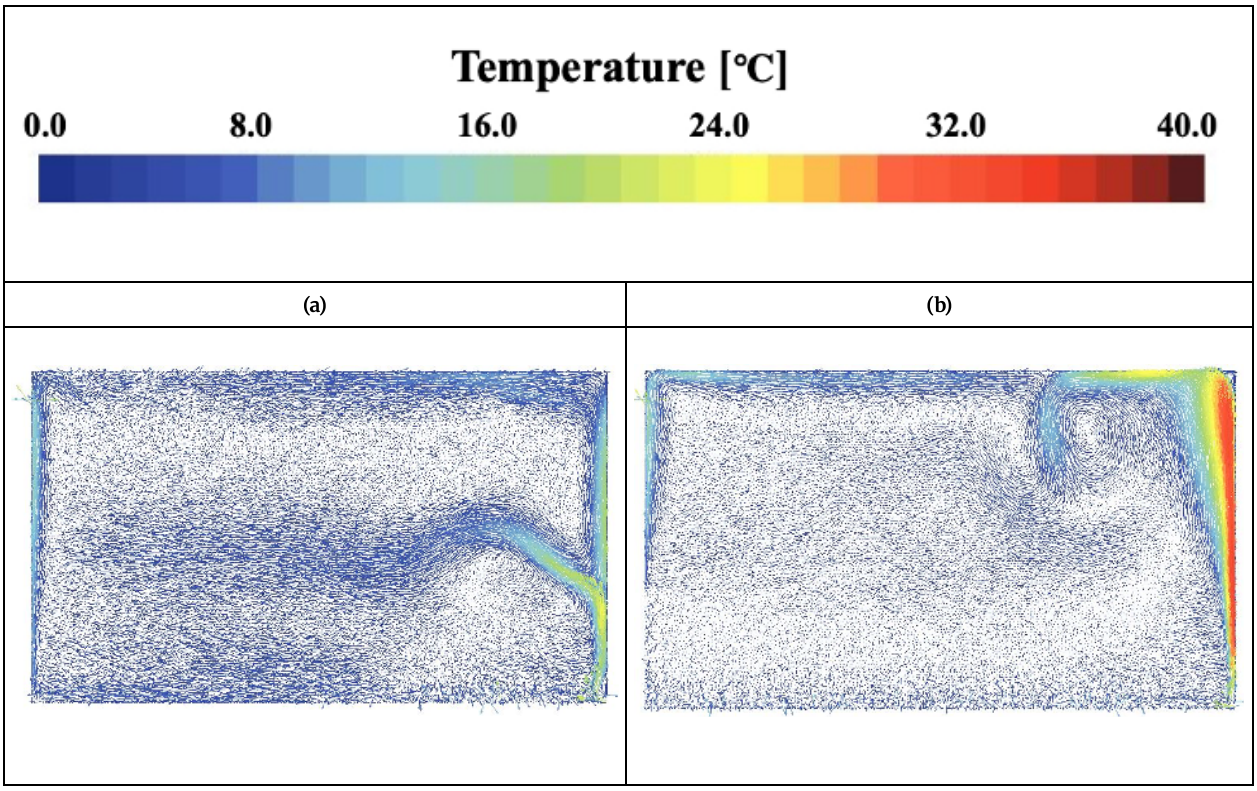

doi.org/10.32388/GV07BN.2

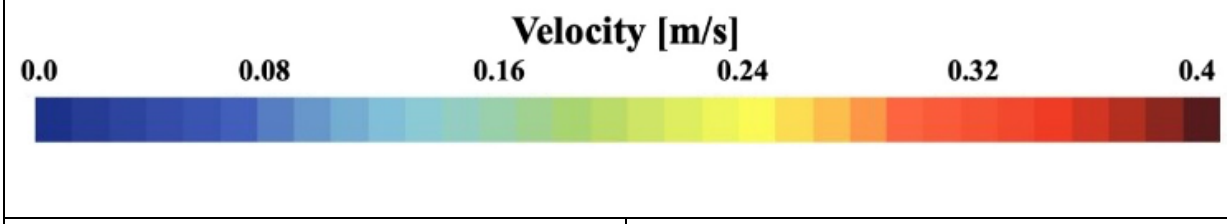

(c)	(d)
	

doi.org/10.32388/GV07BN.2

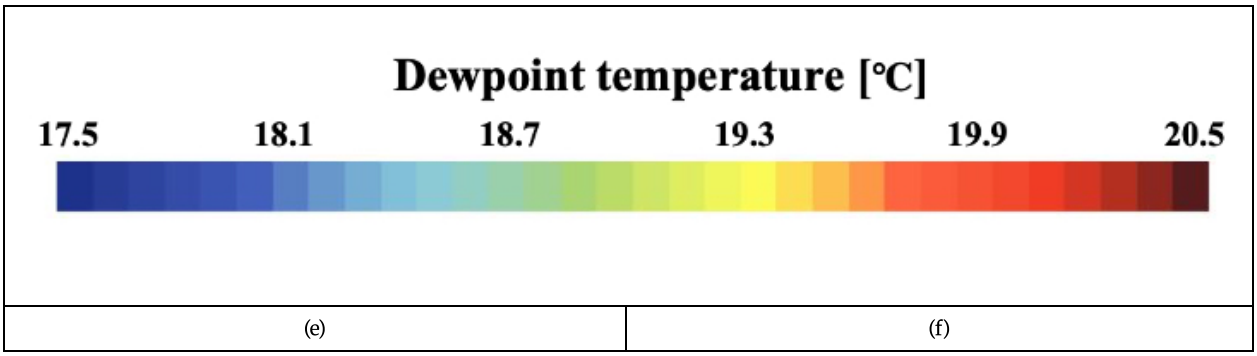

(e)	(f)

Figure 8. Analysis of elements for Cases 2-1-1 and 2-2-1 based on dew condensation risk evaluation of the two-room building with and without a city block. Temperature distribution of the two-room building (a) without a city block and (b) with a city block. Velocity distribution of the two-room building (c) without a city block and (d) with a city block. Dew point temperature distribution of the two-room building (e) without a city block and (f) with a city block.

doi.org/10.32388/GV07BN.2

	

doi.org/10.32388/GV07BN.2

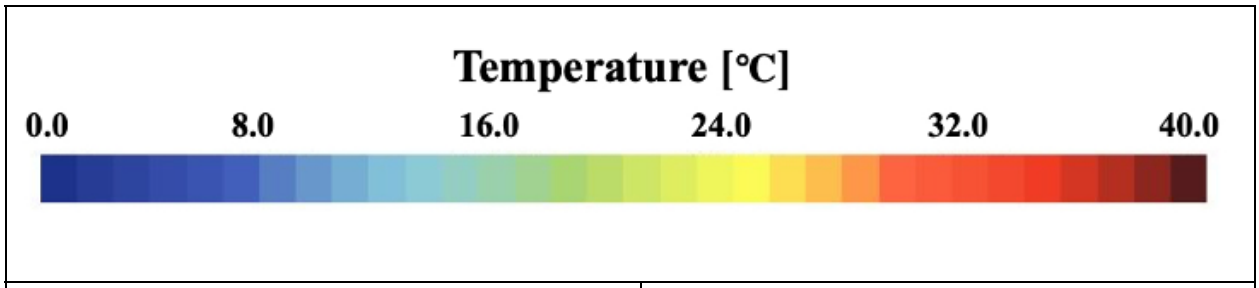

(a)	(b)

doi.org/10.32388/GV07BN.2

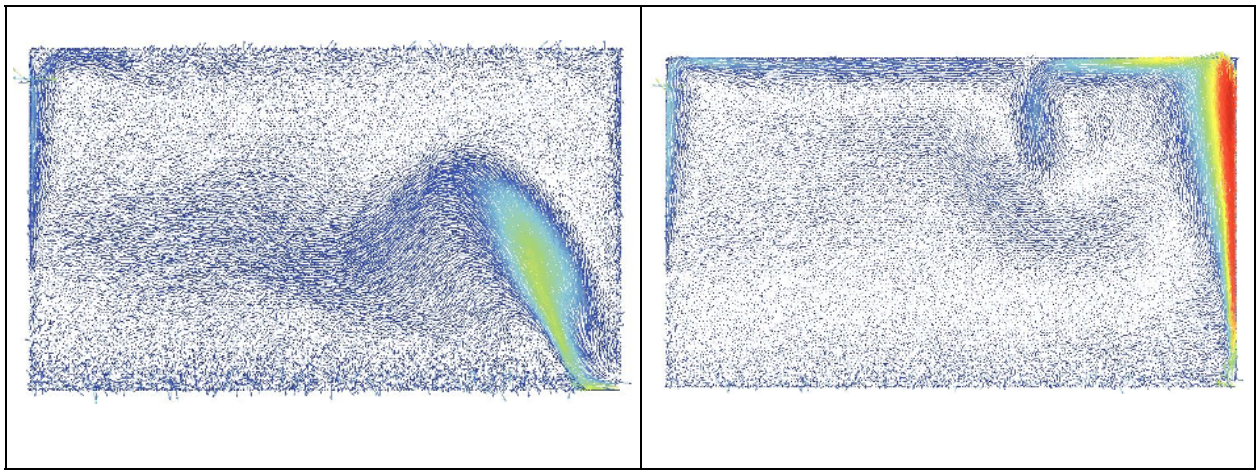

doi.org/10.32388/GV07BN.2

(c)	(d)

doi.org/10.32388/GV07BN.2

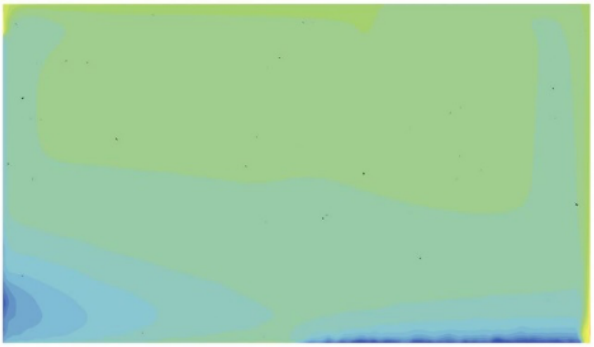

doi.org/10.32388/GV07BN.2

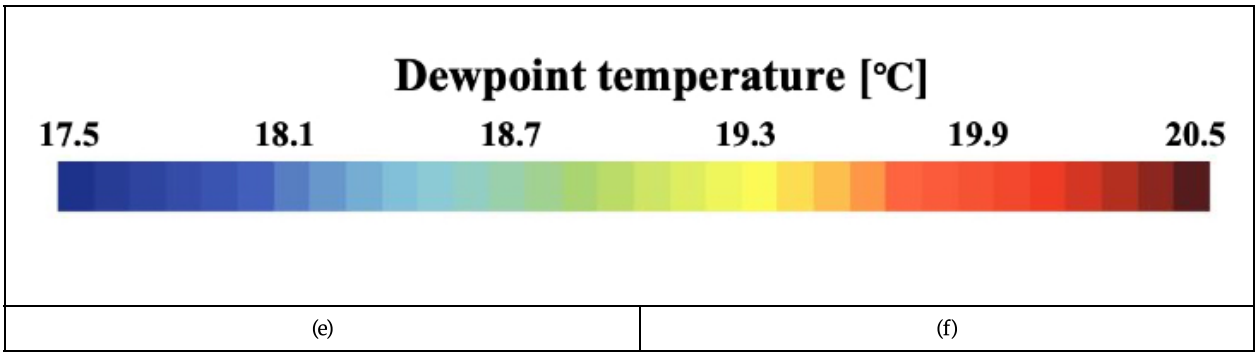

Figure 9. Analysis of elements for Cases 2-1-1 and 2-2-1 based on dew condensation risk evaluation of the one-room building with and without a city block. Temperature distribution of the one-room building (a) without a city block and (b) with a city block. Velocity distribution of the one-room building (c) without a city block and (d) with a city block. Dew point temperature distribution of the one-room building (e) without a city block and (f) with a city block.

Conclusion

In this study, we conducted a basic investigation to examine how differences in the conditions of the target building (with or without a city block) affect ES-CFD coupled analysis. The study focused on the convective heat transfer coefficients and room temperatures, while the influence of outdoor disturbances was fixed. The findings are summarised as follows:

The results showed that the convective heat transfer coefficients influenced the room temperature. Calculations should therefore be performed using CFD, as it provides precise calculations by constantly considering the cost of analysis. In this case, the calculation based on the boundary layer theory was not sufficiently precise because the bulk temperature of the space was set as a reference temperature. In this study, no analysis load was added because the convective heat transfer coefficients were calculated later.

We confirmed that a dew condensation risk evaluation could be conducted in the design phase by calculating the dew point temperature distribution. Because the expanded AMeDAS weather data were used for outdoor air temperature and humidity, which did not reflect the influence of the microclimate, a CFD analysis of the outdoor conditions was necessary for conducting a precise analysis. However, when conducting a simply adequate evaluation, it is not necessary to analyse the city block using CFD. This study indicates the scope of application of the ES-CFD coupled analysis by including a city block.

Limitation

The study was limited by the fact that the influence of transmissive heat flow due to the outdoor microclimate was not reflected. In this respect, the reference temperature for each wall should preferably be changed. The major achievement of this study was that the comparative assessment was conducted using a central value for the outdoor temperature. Therefore, this study was not based on the assumption of a complicated city block, and it considers the role of fundamental data in practical applications.

Future Research

The future prospects are summarised as follows: in addition to conducting a coupled outdoor CFD analysis, it is necessary to develop a method to reduce the calculation load against the variability of the convective heat transfer coefficient over time. CFD analysis should also be developed using a device that considers temporal variability and microclimate.

Statements and Declarations

Funding

Part of this study was supported by the Obayashi Foundation Scholarly Research Support No. 67 of fiscal year 2019.

Declaration of conflicting interests

The authors declare that there are no conflicts of interest.

References

1. ^*He Y, Ren C, Mak HWL, Lin C, Wang Z, Fung JC, Li Y, Lau AK, Ng E (2021). "Investigations of high-density urban bo undary layer under summer prevailing wind conditions*

with Doppler LiDAR: A case study in Hong Kong." Urban Climate. 38: 100884.

2. ^*Zou J, Yu Y, Liu J, Niu J, Chauhan K, Lei C (2021). "Field measurement of the urban pedestrian level wind turbulence". Building and Environment. 194: 107713.*
3. ^*Igoe DP, Downs NJ, Parisi AV, Amar A (2020). "Evaluation of shade profiles while walking in urban environments: A case study from inner suburban Sydney, Australia." Building and Environment. 177: 106873.*
4. ^*Chen C, Chew LP, Gorlé C (2023). "Characterizing spatial variability in the temperature field to support thermal model validation in a naturally ventilated building." Journal of Building Performance Simulation. 16(4): 477-492. doi: 10.1080/19401493.2023.2179115.*
5. ^*Gilbey SE, Reid CM, Zhao Y, Soares MJ, Rumchev KB (2023). "Factors affecting indoor environmental air quality of non-smoking residences in Perth, Western Australia." Indoor and Built Environment. (Ahead of print). doi:10.1177/1420326X221149288.*
6. ^*Tsoulou I, He R, Senick J, Mainelis G, Andrews CJ (2023). "Monitoring summertime indoor overheating and pollutant risks and natural ventilation patterns of seniors in public housing." Indoor and Built Environment. 32(5): 992-1019. doi:10.1177/1420326X221148728.*
7. ^*Lee JH, Kim H, Kim H, Yu KH (2023). "Factors to consider in the performance evaluation of an air purifier using an airborne virus (Phi-X174) in a large chamber." Indoor and Built Environment. 32(6): 1140-1151. doi:10.1177/1420326X231151863.*
8. ^*Luo M, Guo J, Feng X, Chen W (2023). "Studying occupant's heat exposure and thermal comfort in the kitchen through full-scale experiments and CFD simulations." Indoor and Built Environment. 32(5): 928-943. doi:10.1177/1420326X221147161.*
9. ^*Chung JH, Kim S, Sohn DK, Ko HS (2022). "Ventilation efficiency according to tilt angle to reduce the transmission of infectious disease in classroom." Indoor and Built Environment. 32(4): 763-776. doi:10.1177/1420326X221135829.*
10. ^*Zhang D, Ortiz MA, Bluyssen PM (2022). "A review on indoor environmental quality in sports facilities: Indoor air quality and ventilation during a pandemic". Indoor and Built Environment. 32(5): 831-851. doi:10.1177/1420326X221145862.*
11. ^*Luo C, Wu Y, Su X, Zou W, Yu Y, Jiang Q, Xu L (2023). "Influence and characteristic of shading on photovoltaic performance of bifacial modules and method for estimating bifacial gain." Building Simulation. (Ahead of print) doi:10.1007/s12273-022-0966-0.*
12. ^*Mousavi S, Rismanchi B, Brey S, Aye L (2023). "Development and validation of a transient simulation model of a full-scale PCM embedded radiant chilled ceiling." Building Simulation. 16: 813-829. doi:10.1007/s12273-023-0985-5.*
13. ^*Carlucci F, Loonen RC, Fiorito F, Hensen JL (2023). "A novel approach to account for shape-morphing and kinetic shading systems in building energy performance simulations." Journal of Building Performance Simulation. 16(3): 346-365.*
14. ^*Li Y, Liu X, Qian F, Niu S (2020). "Research on the wind environment and air quality of parallel courtyards in a university campus." Sustainable Cities and Society. 56: 102019.*
15. ^*Wu Y, Gao N, Niu J, Zang J, Cao Q (2021). "Numerical study on natural ventilation of the wind tower: Effects of combining with different window configurations in a low-rise house". Building and Environment. 188: 107450.*
16. ^*Zhou Q, Ooka R (2021). "Influence of data preprocessing on neural network performance for reproducing CFD simulations of non-isothermal indoor airflow distribution". Energy and Buildings. 230: 110525.*
17. ^*Mirzaei PA (2021). "CFD modeling of micro and urban climates: Problems to be solved in the new decade." Sustainable Cities and Society. 69: 102839.*
18. ^*Okaze T, Kikumoto H, Ono H, Imano M, Ikegaya N, Hasama T, Nakao K, Kishida T, Tabata Y, Nakajima K, Yoshie R, Tominaga Y (2021). "Large-eddy simulation of flow around an isolated building: A step-by-step analysis of influencing factors on turbulent statistics." Building and Environment. 202: 108021.*
19. ^*Alajmi AF, Abou-Ziyan HZ, El-Amer W (2013). "Energy analysis of under-floor air distribution (UFAD) system: An office building case study." Energy Conversation and Management. 73: 78–85.*
20. ^*Zhai Z, Chen Q, Haves P, Klems JH (2002). "On approaches to couple energy simulation and computational fluid dynamics programs". Building and Environment. 37: 857–864.*
21. ^*Zhai Z, Chen Q (2003). "Solution characters of coupling between energy simulation and CFD programs". Energy and Buildings. 35(5): 493–505.*
22. ^*Zhai Z, Chen Q (2005). "Performance of coupled building energy and CFD simulation". Energy and Buildings. 37 (4): 333–344.*
23. ^*Barbason M, Reiter S (2014). "Coupling building energy simulation and computational fluid dynamics: Application to a two-story house in a temperate climate." Building and Environment. 75: 30–39.*
24. ^*Fan Y, Ito K (2012). "Energy consumption analysis intended for real office space with energy recovery ventilator by integrating BES and CFD approaches." Building and Environment. 52: 57–67.*
25. ^*Fan Y, Ito K (2014). "Integrated building energy computational fluid dynamics simulation for estimating the energy-saving effect of energy recovery ventilator with CO2 demand-controlled ventilation system in office space." Indoor and Built Environment. 23(6): 785–803.*

26. ^ *Aghamolaei R, Fallahpour M, Mirzaei PA (2021). "Temp o-spatial thermal comfort analysis of urban heat island with coupling of CFD and building energy simulation." E nergy and Buildings. 251: 111317.*
27. ^ *Shan X, Luo N, Sun K, Hong T, Lee YK, Lu WZ (2020). "Co upling CFD and building energy modelling to optimize th e operation of a large open office space for occupant comf ort." Sustainable Cities and Society. 60: 102257.*
28. ^ *Piscia D, Muñoz P, Panadès C, Montero JI (2015). "A meth od of coupling CFD and energy balance simulations to stu dy humidity control in unheated greenhouses." Computer s and Electronics in Agriculture. 115: 129–141.*
29. ^ *Zhang R, Mirzaei PA, Jones B (2018). "Development of a dynamic external CFD and BES coupling framework for a pplication of urban neighbourhoods energy modelling". B uilding and Environment. 146: 37–49.*
30. ^ *Zhang R, Mirzaei PA (2021). "Fast and dynamic urban n eighbourhood energy simulation using CFDf-CFDc-BES c oupling method". Sustainable Cities and Society. 66: 1025 45.*
31. ^ *Kawai H, Asawa T, Hoyano A (2013). "Numerical analysi s on the effect of the outdoor thermal radiation environm ent on the performance of a direct gain system." Journal o f Environmental Engineering (New York). 78(693): 841–84 8.*
32. ^ *TRNSYS (2019) What is TRNSYS? http://www.trnsys.co m/ (accessed 20 December 2021).*
33. ^ *Pulkkinen J, Louis JN (2021). "Near- and medium-term h ourly morphed mean and extreme future temperature da tasets for Jyväskylä, Finland, for building thermal energy demand simulations." Data in Brief. 37: 107209.*
34. ^ *Arima Y, Ooka R, Kikumoto H, Yamanaka T (2015). "A pr ototype of near future standard weather data and the im pact of climate change on building energy load in kanto r egion in summer: Making future weather data for buildin g energy simulation by dynamical downscaling (Part 1)." Journal of Environmental Engineering (New York). 80(71 0): 371–379.*
35. ^ *Kikumoto H, Ooka R, Arima Y (2016). "A study of urban t hermal environment in Tokyo in summer of the 2030s un der influence of global warming." Energy and Buildings. 1 14: 54–61.*
36. ^ *Tang Y, Sun T, Luo Z, Omidvar H, Theeuwes N, Xie X, Xio ng J, Yao R, Grimmond S (2021). "Urban meteorological fo rcing data for building energy simulation." Building and Environment. 204: 108088.*
37. ^ *Yamamoto T, Ozaki A, Kaoru S, Taniguchi K (2021). "Ana lysis method based on coupled heat transfer and CFD sim ulations for buildings with thermally complex building en velopes". Building and Environment. 191: 107521.*
38. ^ *Digital Agency. (1954) Article 54, The Building Standard Law. E-Gov Horei Kensaku (Search engine for legal docu ments), https://elaws.e-gov.go.jp/document?lawid=325AC 0000000201 (Accessed 23 February 2022. In Japanese).*
39. ^ *SIEMENS. Simcenter STAR-CCM+: Engineer innovation with CFD- focused multiphysics simulation, https://www. plm.automation.siemens.com/global/ja/products/simcent er/STAR-CCM.html (accessed 20 December 2021. In Japan ese).*
40. ^ *Lien FS, Chen WL, Leschziner MA (1996). "Low-Reynold s number eddy-viscosity modelling based on non-linear s tress-strain/vorticity relations." Proc. 3rd Symp. on Engin eering Turbulence Modelling and Measurements, 27-29 C rete, Greece.*

Declarations

Funding: Part of this study was supported by the Obayashi Foundation Scholarly Research Support No. 67 of fiscal year 2019.

Potential competing interests: No potential competing interests to declare.